

*Citation for published version:*

Ciampa, F & Meo, M 2010, A new wavelet based algorithm for impact identification and group velocity determination in composite structures. in *Proceedings of the 5th European Workshop - Structural Health Monitoring 2010*. pp. 1057-1063, 5th European Workshop on Structural Health Monitoring, Sorrento, Italy, 28/06/10.

*Publication date:*  
2010

*Document Version*  
Early version, also known as pre-print

[Link to publication](#)

**University of Bath**

## **Alternative formats**

If you require this document in an alternative format, please contact:  
[openaccess@bath.ac.uk](mailto:openaccess@bath.ac.uk)

### **General rights**

Copyright and moral rights for the publications made accessible in the public portal are retained by the authors and/or other copyright owners and it is a condition of accessing publications that users recognise and abide by the legal requirements associated with these rights.

### **Take down policy**

If you believe that this document breaches copyright please contact us providing details, and we will remove access to the work immediately and investigate your claim.

**Cover page**

**Title: A NEW WAVELET BASED ALGORITHM FOR IMPACT  
IDENTIFICATION AND GROUP VELOCITY DETERMINATION IN  
COMPOSITE STRUCTURES**

**Authors: Francesco Ciampa  
Michele Meo**

## Abstract

This paper presents a new *in-situ* Structural Health Monitoring (SHM) concept able to identify the source of acoustic emission and to determine the group velocity in complex composite structures with unknown lay-ups and thicknesses. The proposed methodology, based on the differences of stress waves measured by surface attached PZT sensors, was divided in two steps. In the first step, the time of arrivals (TOA) of the wave packets were determined by a joint time frequency analysis based on the magnitude of the Continuous Wavelet Transform (CWT) squared modulus. Then, the coordinates of the impact location and the wave speed were obtained by solving a set of non-linear equations through a combination of global Line Search and backtracking techniques associated to a local Newton's iterative method. The proposed method overcomes the limitations of a triangulation algorithm as it does not require *a priori* knowledge of the wave group speed, even for complex angular group velocity patterns, as in anisotropic and inhomogeneous materials. To validate this algorithm, experimental tests were conducted on two different composite structures, a quasi-isotropic CFRP and a sandwich panel. The results showed that the impact source location and the group speed were predicted with reasonable accuracy (maximum error in estimation of the impact location was approximately 2% for quasi-isotropic CFRP panel and nearly 1% mm for sandwich plate), requiring little computational time (less than 2 s).

## 1. Introduction

In the last decade, a number of studies present in literature were focused on the *in-situ* low-velocity impact source identification on both aluminum [3, 4, 6] and composite plates [9, 10, 13] using a network of piezoelectric (PZT) transducers. For isotropic or quasi-isotropic materials, a time of arrival triangulation technique (also known as Tobias algorithm) was widely used for determining the source location. In this approach, the impact point was identified as the intersection of three circles, whose centers were the sensors location [15]. Ciampa and Meo [1] proposed a Newton-based optimization technique for the impact point localization and flexural

---

<sup>1</sup> Francesco Ciampa, Michele Meo, Material Research Centre, Department of Mechanical Engineering, University of Bath, Bath BA27AY, UK

group velocity determination, based on the time differences of stress waves measured by four surface-attached PZT transducers. However, in these methods the wave velocity is assumed constant in all directions, which is not true in anisotropic and inhomogeneous materials. Paget et al. [12] and Kurokawa et al. [7] developed an algorithm for impact location based on elliptical group velocity pattern. This method requires the knowledge of the group velocities at 0 and 90 degrees with respect to the planar reference frame, and it can be used for quasi-isotropic and unidirectional composite plates. However, the acoustic emission source location in composite structures, with complex angular group-velocity pattern, remains a challenging task that still need to be solved. This research work presents a new *in-situ* Structural Health Monitoring (SHM) system able to identify low-velocity impact and acoustic emission sources and to determine the flexural Lamb mode ( $A_0$ ) velocity in complex composite structures with unknown lay-up and thickness. The proposed algorithm is based on the differences of the waves packets measured by six surface attached acoustic emission PZT sensors. A joint time-frequency analysis based on the magnitude of the Continuous Wavelet Transform (CWT) squared modulus was employed for the time of arrivals (TOA) of the stress waves. Then, the coordinates of the impact location and the group speed were obtained by solving a set of non-linear equations through a combination of local Newton's iterative method associated to a global unconstrained optimization (Line Search and backtracking techniques). Therefore, the proposed method overcomes the drawbacks of a triangulation algorithm and it does not require an *a-priori* knowledge of the anisotropy group speed of the AE signals. To validate this algorithm, experimental location testing were conducted on two different composite structures, a quasi-isotropic CFRP laminate and a sandwich panel.

## 2. Acoustic source localization algorithm

Let us consider as origin of the planar reference frame the left bottom corner of the composite structure. The impact source point  $I$  is at unknown coordinates  $(x_I, y_I)$  in the plane of the plate, the transducers are located at distance  $l_i$  ( $i=1, \dots, 6$ ) from the source, and  $d_{kj}$  ( $k=1,3,5$ ) ( $j=2, \dots, 6$ ) is the distance between each pair of transducers  $k$  and  $j$  (Fig. 1). Furthermore, the dimensions of the plate are  $L$ , length and  $W$ , width.

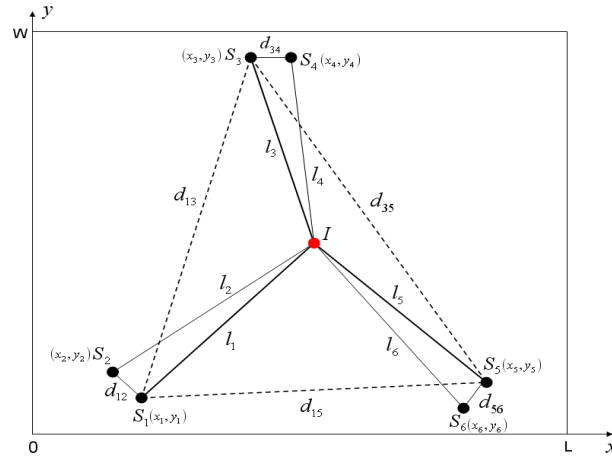


**Figure 1** Sensors arrangement for the source location

The coordinates of the acoustic emission source can be determined by solving the following equation:

$$(x_i - x_I)^2 + (y_i - y_I)^2 - (t_i V_{g,i})^2 = 0 \quad (2.1)$$

where  $V_{g,i}$  is the velocity of propagation of the stress wave reaching the  $i$ -th transducer,  $t_i$  is the time of detection of the AE signals and  $(x_i, y_i)$  are the coordinates of the  $i$ -th sensor. Equation (2.2) represents a system of six equations for 14 unknowns ( $t_i$ ,  $x_I$ ,  $y_I$  and  $V_{g,i}$ ), however, if  $t_1$  is the travel time required to reach the sensor 1 (*master sensor*) and  $\Delta t_{1j}$  ( $j = 2, \dots, 6$ ) are the time difference between sensor  $j$  and 1, we can write:

$$t_j = t_1 \pm \Delta t_{1j} \quad (2.2)$$

Substituting equation (2.2) into (2.1), we obtain:

$$(x_i - x_I)^2 + (y_i - y_I)^2 - [(t_1 \pm \Delta t_{1j}) V_{g,i}]^2 = 0 \quad (2.3)$$

The above set of nonlinear equations cannot be solved since the number of variables is still bigger than the number of equations. Thereby, in order to find a solution of system (2.3), additional information is needed, i.e. an optimal sensors configuration. In the current approach, the sensors were disposed in way that each pair of transducers was relatively close together. In this manner, any pair will experience approximately the same group velocity (see Fig. 1). Therefore, we have straightaway that  $V_{g,1} \approx V_{g,2}$ ,  $V_{g,3} \approx V_{g,4}$ ,  $V_{g,5} \approx V_{g,6}$  and the system (2.3) can be rewritten as:

$$(x_i - x_I)^2 + (y_i - y_I)^2 - [(t_1 \pm \Delta t_{1j}) V_{g,k}]^2 = 0 \text{ with } k = 1, 3, 5 \quad (2.4)$$

Source location and group velocity of the flexural Lamb mode can now be calculated by solving the above set of six nonlinear equations with the six unknowns  $\mathbf{x} = \{x_I, y_I, t_1, V_{g,1}, V_{g,3}, V_{g,5}\}$ . Therefore, since no wave velocity relationship with the heading angle is required, the proposed technique is able to obtain the source location in anisotropic or complex structures for arbitrary lay-up or thickness of the plate.

### 3. Time of arrival identification using the Continuous Wavelet Transform

The Continuous Wavelet Transform (CWT) is a linear transform that correlates the harmonic waveform  $u(x, t)$  with basis functions that are simply dilatations and translations of a mother wavelet  $\psi(t)$ , by the continuous convolution of the signal and the scaled or shifted wavelet [8]:

$$WT(x, a, b) = \frac{1}{\sqrt{a}} \int_{-\infty}^{+\infty} u(x, t) \psi^* \left( \frac{t-b}{a} \right) dt \quad (3.1)$$

where  $\psi^*(t)$  denotes the complex conjugate of the mother wavelet  $\psi(t)$ ,  $a$  is the dilatation or scale parameter defining the support width of the wavelet and  $b$  the translation parameter localizing the wavelet in the time domain. In this study complex Morlet wavelet was used as it is able to separate amplitude and phase, enabling the

measurement of instantaneous frequencies and their temporal evolution [14]. The waveforms recorded are analyzed in terms of group (energy) velocity–frequency relationship. Let us assume a time harmonic motion of two waves of unit amplitude with different frequencies  $\omega_1$  and  $\omega_2$  propagating in the x-direction of a thin plate as follow:

$$u(x, t) = e^{-j(k_1 x - \omega_1 t)} + e^{-j(k_2 x - \omega_2 t)} \quad (3.2)$$

where  $k_1$  and  $k_2$  are the wave numbers. Substituting equation (3.2) in (3.1) using complex Morlet wavelet and assuming  $\vartheta_1 = \omega_1 b - k_1 x$  and  $\vartheta_2 = \omega_2 b - k_2 x$ , we have:

$$WT(x, a, b) = \sqrt{a} [\hat{\psi}^*(a\omega_1) e^{j\vartheta_1} + \hat{\psi}^*(a\omega_2) e^{j\vartheta_2}] \quad (3.3)$$

The squared modulus of the CWT called also *scalogram* indicates the energy density of the signal at each scale at any time [5, 8]. Hence, it is able to reveal the highest local energy content of the waveform  $u(x, t)$  measured from each transducer. The squared modulus can be express as:

$$|WT(x, a, b)|^2 = WT(x, a, b) \cdot WT^*(x, a, b) \quad (3.4)$$

Substituting equations (3.3) and its complex conjugate into (3.4), if  $\Delta\omega$  is sufficiently small such that  $\hat{\psi}(a\omega_1) \cong \hat{\psi}(a\omega_2) \cong \hat{\psi}(a\omega_0)$ , we obtain:

$$|WT(x, a, b)|^2 \approx 2a [\hat{\psi}(a\omega_0)]^2 [1 + \cos(\Delta\omega b - \Delta k x)] \quad (3.5)$$

Equation (3.5) shows that the squared modulus of the CWT using complex Morlet wavelet reaches its peak value at  $a = \frac{\omega_c}{\omega_0}$  and  $b = \frac{\Delta k}{\Delta\omega} x = \frac{x}{V_g}$ . Hence, the angular

frequency of interest  $\omega_0$ , corresponding at the maximum value of the Continuous Wavelet Transform squared modulus coefficients (ridges), allows identifying the arrival time of the group velocity  $V_g$  (Fig. 2).

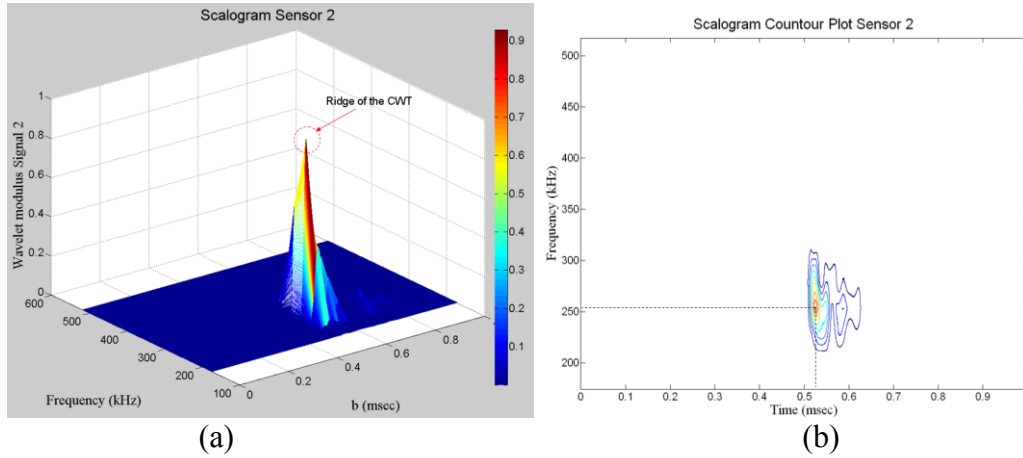


**Figure 2 (a) (b)** Morlet wavelet scalogram (a) and associated contour plot (b) of the recorded flexural wave.

As depicted in figure (2-a), a red patch in the scalogram is representative of the ridge, i.e. the local energy content of the waveform recorded. Figure (2-b) shows that the projection on the time domain of the ridge corresponds to the time of arrival (TOA) of the waves packets.

#### 4. Optimization algorithm for solving systems of non-linear equations

The method adopted for solving the set of equations (2.4) was to combine a Newton's method with an unconstrained optimization. Analogously to Ciampa and Meo [1], the set of non linear equations (2.4) can be expressed as:

$$\mathbf{F}(\mathbf{x}) = 0 \quad (4.1)$$

where  $\mathbf{F}$  is the vector of the functions  $F_i$  ( $i=1,\dots,6$ ) and  $\mathbf{x}$  is the vector of unknowns  $x_j$  ( $j=1,\dots,6$ ). However, in particular conditions, Newton's method may not converge [11]. The reasons for this failure are that the direction of the current iterate  $\mathbf{x}^n$  might not be a direction of descent for  $\mathbf{F}$ , and, even if a search direction is a direction of decrease of  $\mathbf{F}$ , the length of the Newton step  $\delta\mathbf{x}$  may be too long. Hence, the approach adopted was to combine the Newton's method applied to the system (2.4) with the unconstrained problem of minimizing the *objective function*  $\mathbf{F}$  [2]:

$$\min_{\mathbf{x} \in \mathfrak{R}^n} \mathbf{F} : \mathfrak{R}^n \rightarrow \mathfrak{R} \quad (4.2)$$

Among the class of powerful algorithms for unconstrained optimization, in this paper we focused on the Line-Search method and the polynomial backtracking technique because of its simplicity, and because they do not depend on how the Jacobian is obtained. In particular, the function to be minimized was the squared norm of the objective function [1]. The computational time for each source location was less than 1 s (using a code written in Matlab), which means that the results can be obtained in quasi real-time using a compiled code.

#### 5. Experimental set-up and source localization results

To validate this algorithm, experimental location testing were conducted on two different composite structures, a carbon fibre reinforced plastic (CFRP) composite laminate with dimensions 502 mm x 437 mm x 6.94 mm and lay-up sequence of [0/15/30/45/60/75/90]<sub>3s</sub>, and a sandwich plate with dimensions of 380 mm long, 254 mm wide and 6.35 mm thick. The  $A_0$  Lamb waves were generated using a hand-held modal hammer and were measured employing six Acoustic Emission sensors surface bonded with a central frequency of 300 kHz, provided by the courtesy of Airbus UK. Transducers location and impact source coordinates are reported in the following tables (1-3) for test 1 with CFRP (referred as impacts C1 and C2 in the article) and for test 2 with sandwich plate (referred as impacts S1 and S2 in the article).

**Table 1** Sensors and impact coordinates in test 1, impacts C1 and C2.

	<i>Sensor 1</i>	<i>Sensor 2</i>	<i>Sensor 3</i>	<i>Sensor 4</i>	<i>Sensor 5</i>	<i>Sensor 6</i>	<i>Impact C1</i>	<i>Impact C2</i>
x-coordinate (mm)	120	110	250	280	430	420	280	270
y-coordinate (mm)	100	120	390	390	250	230	170	240

**Table 2** Sensors and impact coordinates in test 2, impact S1

	<i>Sensor 1</i>	<i>Sensor 2</i>	<i>Sensor 3</i>	<i>Sensor 4</i>	<i>Sensor 5</i>	<i>Sensor 6</i>	<i>Impact S1</i>
x-coordinate (mm)	120	110	190	210	320	330	210
y-coordinate (mm)	50	70	210	190	140	120	90

**Table 3** Sensors and impact coordinates in test 2, impact S2

	Sensor 1	Sensor 2	Sensor 3	Sensor 4	Sensor 5	Sensor 6	Impact S2
x-coordinate (mm)	100	90	170	190	310	290	190
y-coordinate (mm)	50	70	220	210	140	120	140

The maxima scalogram coefficients were found at the instantaneous frequency of 258.77 kHz in the experiments with the quasi-isotropic CFRP plate and 348.27 kHz with the sandwich structure. Figure 3 illustrates the line profiles of the scalogram at the above frequencies of interest, for the configurations reported in test 1, impact C1 and test 2, impact S1.

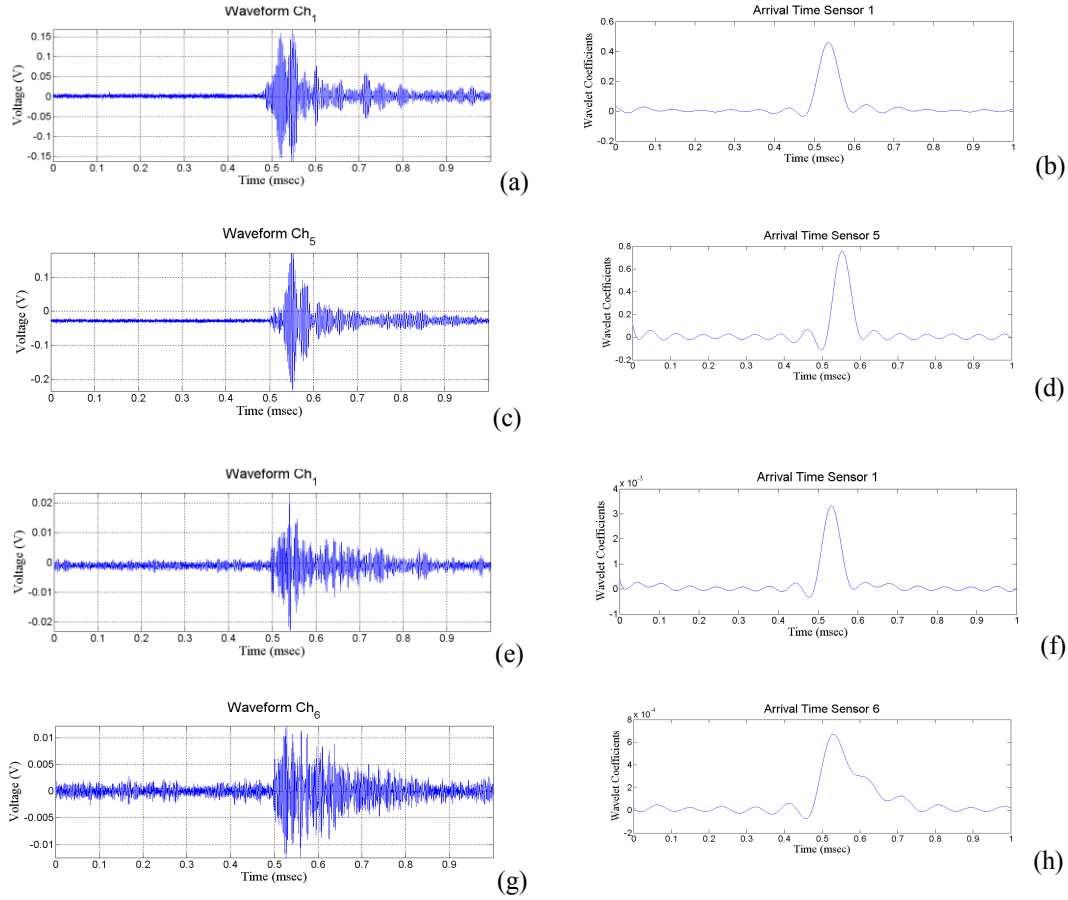


**Figure 3** Time histories of the recorded waveform for impact C1 (a and c) and S1 (e and g) and procedure for the TOA identification for impact C1 (b and d) and S1 (f and h).

Table 4 depicts the true and evaluated impact positions and the error as expressed by the error function  $\psi = \sqrt{(x_{real} - x_{calculated})^2 + (y_{real} - y_{calculated})^2}$ . Table 5 provides the values of the fundamental flexural Lamb mode measured from any pair of sensors.

**Table 4** Impact positions and errors for test 1 and 2

	Impact C1	Impact C2	Impact S1	Impact S2
x-coordinate source location (from algorithm)	277.56 mm	268.32 mm	211.71 mm	188.23 mm
x-coordinate source location (real value)	280 mm	270 mm	210 mm	190 mm
y-coordinate source location (from algorithm)	172.43 mm	242.12 mm	89.18 mm	141.07 mm
y-coordinate source location (real value)	170 mm	240 mm	90 mm	140 mm
Location error $\psi$	3.44 mm	2.7 mm	1.89 mm	2.07 mm



**Table 5** Flexural Lamb mode wave velocity results for test 1 and 2

		Impact C1	Impact C2	Impact S1	Impact S2
Group velocity (from algorithm)	Sensors 1-2 (m/s)	1618.32	1617.22	2810.08	2768.15
	Sensors 3-4 (m/s)	1624.56	1622.12	3200.23	3078.86
	Sensors 5-6 (m/s)	1616.44	1619.78	2840.74	2924.43

As it can be seen from the above tables, this algorithm provides results with satisfactory accuracy (maximum error in estimation of the coordinates of the impact location was nearly 3 mm for CFRP plates and approximately 2 mm in complex structures as sandwich panels). In addition, according to the quasi-isotropic nature of the CFRP composite plate, all the group velocities of the  $A_0$  Lamb mode measured by any pair of transducers were approximately the same (close to the limit value of 1620 m/s).

## Conclusions

This research work has shown a new *in-situ* Structural Health Monitoring (SHM) method for locating acoustic emission source and for determining the velocity of flexural waves in complex composite structures. The proposed method is based on the differences of the stress waves measured by six surface attached acoustic emission PZT sensors. The Continuous Wavelet Transform (CWT) scalogram, which guarantees high accuracy in the time-frequency analysis of the acoustic waves, was employed to identify the arrival time (TOA) of the flexural  $A_0$  Lamb mode. The coordinates of the impact location and the group speed were obtained by solving a set of non-linear equations through a combination of local Newton's iterative method associated to Line Search and backtracking techniques. This algorithm does not require *a priori* knowledge of the anisotropy group velocity of the AE waveforms as well as the lay-up and thickness of the structure. The experimental results conducted on a quasi-isotropic CFRP laminate and a sandwich panel showed that source location was achieved with satisfactory accuracy (maximum error in estimation of the impact location was approximately 3 mm for quasi-isotropic CFRP panel and nearly 2 mm for sandwich plate).

## References

- [1] Ciampa F, Meo M. *Smart material and Structures*, **19**, 2010, pp. 1-14
- [2] Dennis J E, Schnabel R B. Englewood Cliffs, NJ: Prentice Hall., 1983
- [3] Gaul L, Hurlbauss S, Jacobs L J. *Research in Nondestructive Evaluation*, **13**, 2001, pp. 105-117
- [4] Gaul L, Hurlbauss S. *Archive of Applied Mechanics*, **69**, 1999, pp. 691-701
- [5] Haase M, Widjajakusuma J. *International Journal of Engineering Science* **41**, 2003, pp. 1423-1443
- [6] Jeong H, Jang Y-S. *IEEE Transaction on Ultrasonics, Ferroelectrics, and Frequency Control*, Vol. 47, No. 3, 2000, pp.612-619
- [7] Kurokawa Y, Mizutani Y, Mayozumi M. *Journal of Acoustic Emission* **23**, 2005, pp. 224-232.
- [8] Mallat S. London: Academic Press, 1998
- [9] Matt H, Lanza di Scalea F. *Smart materials and Structures*, **16**, 2007, pp. 1489-1499.
- [10] Meo M, Zumpano G, Pigott M, Marengo G. *Composite Structures* **71**, 2005, pp. 302-306
- [11] Nocedal J, Wright S J. *Proceeding of the 4<sup>th</sup> International Workshop on Structural Health Monitoring, Stanford, CA*, 2003, pp. 363-370
- [12] Sung D U, Oh J H, Kim C G, Hong C S. *Journal of Intelligent Material Systems*, Vol. 11, 2000, pp. 180-190
- [13] Teolis A. Birkhauser, Boston, 1998.
- [14] Tobias A. *Non-Destructive Testing*, Vol. 9, No. 1, 1976, pp. 9-12